Stability of Continuous Double-Plate Systems

V. X. Kunukkasseril* and A. S. J. Swamidas†
Indian Institute of Technology, Madras, India

Stability characteristics of circular double-plate systems which are interconnected by n intermediate, concentric, and elastic ring supports are considered in this paper. In particular, for annular isotropic plates with different loads at the inner and outer edges, closed-form solutions in terms of integrals of Bessel and Lommel functions are developed for the symmetric ($m=0$) and the first asymmetric ($m=1$) modes. Also, it is shown that, for isotropic complete plates and annular plates with equal loads at the inner and outer edges, the solutions will reduce to the well-known solutions in terms of Bessel functions. Several new buckling characteristics of the continuous double-plate systems are illustrated by numerical results obtained for isotropic, fixed-fixed, and fixed-free systems with one intermediate elastic connection.

Nomenclature

a = outer radius of the top plate
a_{il} = inner radius of the top plate
A_1 = $[\sigma_{0l}-\sigma_{il}(a_{il}/a)^2]/[1-(a_{il}/a)^2]$, for the top plate
A_2 = $[(\sigma_{0l}-\sigma_{il})/\{1-(a_{il}/a)^2\}]\,(a_{il}/a)^2$, for the top plate
b = outer radius of the bottom plate
b_{i2} = inner radius of the bottom plate
d = b/a
D_1 = $E_1 h_1^3/12(1-\nu_1^2)$, flexural stiffness of the top plate in the radial direction
D_2 = $E_2 h_2^3/12(1-\nu_2^2)$, flexural stiffness of the bottom plate in the radial direction
E_1, E_2 = Young's moduli of elasticity of the top and bottom isotropic plates
h_1, h_2 = thickness of the top and bottom plates
$J_\beta(\mu^{1/2}\rho)$, $Y_\beta(\mu^{1/2}\rho)$ = Bessel functions of the first and and second kind of order β and argument $(\mu^{1/2}\rho)$
$K_1, K_2, \ldots K_j \ldots K_n$ = linear elastic stiffnesses of the intermediate and edge supports in force-/unit deflection/unit length
M_ρ = moment per unit length in the radial direction
n = total number of annular and complete circular plate segments
N_1 = $h_1\sigma_{01}$, the in-plane, radial, compressive force applied at the outer edge of the top plate
N_{il} = $h_1\sigma_{il}$, the in-plane, radial, compressive force applied at the inner edge of the top plate
N_2 = $h_2\sigma_{02}$, the in-plane, radial compressive force applied at the outer edge of the bottom plate
N_{i2} = $h_2\sigma_{i2}$, the in-plane radial, compressive force applied at the inner edge of the bottom plate
q = $K_1 a^3/D_1$, the coefficient of support elasticity
Q_ρ = radial shear force per unit length
r, ρ = dimensional and nondimensional radial distances
s = number of nodal circles
s_1 = $E_1(1-\nu_2^2)/E_2(1-\nu_1^2)$
V_r, V_ρ = dimensional and nondimensional Kirchhoff shear force per unit width
$w_1, w_2, \bar{w}_1, \bar{w}_2$ = dimensional and nondimensional deflection of the top and bottom plates
∇^2 = $\dfrac{\partial^2}{\partial\rho^2}+\dfrac{1}{\rho}\dfrac{\partial}{\partial\rho}+\dfrac{1}{\rho^2}\dfrac{\partial^2}{\partial\theta^2}$
θ = tangential coordinate
κ_j = K_j/K_1
μ = $N_1 a^2/D_1$
μ_2 = $N_2 b^2/D_2$
μ_{1j} = $(A_1 h_1 a^2)/D_1$
μ_{2j} = $(A_2 h_1 a^2)/D_2$
ν_1, ν_2 = Poisson's ratio of the top and bottom plates
ρ = r/a
ρ_s = b_1/a
ρ_{s1} = b_1/b
$\sigma_{\rho j1}, \sigma_{\theta j1}, \tau_{\rho\theta j1}$ = radial and tangential normal and shear stresses occurring at the jth segment of the top continuous plate
σ_{j-1}, σ_j = in-plane radial stresses existing in the continous plate at the $(j-1)^{\text{th}}$ and j^{th} supports
σ_{01}, σ_{02} = applied in-plane, radial stresses at the outer edge of top and bottom plates
σ_{i1}, σ_{i2} = applied in-plane, radial stresses at the inner edge of the top and bottom plates

Received August 16, 1974; revision received March 25, 1975.
Index category: Structural Stability Analysis.
*Department of Applied Mechanics.
*Professor, Department of Applied Mechanics.
†Lecturer, Department of Applied Mechanics.

Introduction

THE stability of rectangular continuous plates has received quite a lot of attention[1-5] during the past four decades, but the stability aspects of continuous circular plates have not been investigated much. Only very recently a paper was published[6] on the stability of continuous plates. In the present work, a further extension of the work reported in Ref. 6 is carried out for the case of the double-plate system shown in Fig. 1. The plates are connected together by linear, elastic, concentric ring supports. These types of systems have applications in designing structures with high strength/weight ratios. In particular, these types of systems are considered to be useful in the design of aerospace structures like space platforms, solar panels, etc.

For the general case of buckling of continuous isotropic plates, Frobenius series solutions have been formulated. For the particular cases of complete isotropic plates and annular isotropic plates with equal in-plane loads at the inner and outer edges, the previous series olutions reduce to available solutions in terms of Bessel functions.[6] Closed-form solutions in terms of Bessel and Lommel functions and their integrals

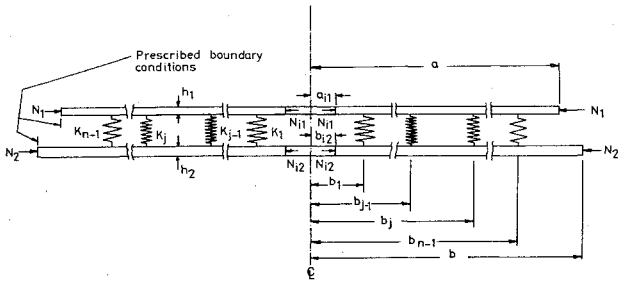

Fig. 1 A continuous double system on $(n-1)$ elastic intermediate ring supports.

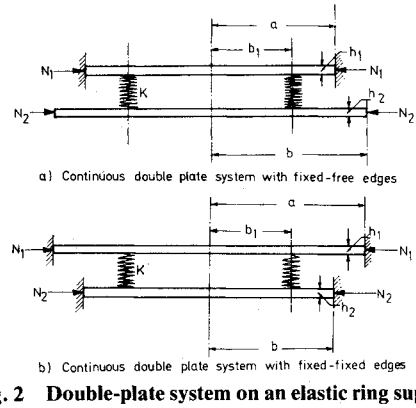

Fig. 2 Double-plate system on an elastic ring support.

are given for the case of symmetric $(m=0)$ and the first asymmetric $(m=1)$ buckling of annular isotropic plates with different loads on the inner and outer edges. Detailed numerical results are given to illustrate the behavior of the two specific types of problem shown in Fig. 2.

Governing Equilibrium Equations and Solutions

The governing nondimensional equation obtained by considering the forces and moments acting on an element of each plate is (top plate)

$$\nabla 4\bar{w}_1 - \frac{a^2}{D_1}\left[N_{\rho 1}\frac{\partial^2\bar{w}_1}{\partial\rho^2}+N_{\theta 1}\left(\frac{1}{\rho}\frac{\partial\bar{w}_1}{\partial\rho}+\frac{1}{\rho^2}\frac{\partial^2\bar{w}_1}{\partial\theta^2}\right)+2N_{\rho\theta 1}\left(\frac{1}{\rho^2}\frac{\partial\bar{w}_1}{\partial\theta}-\frac{1}{\rho}\frac{\partial^2\bar{w}_1}{\partial\rho\,\partial\theta}\right)\right]=0 \tag{1}$$

Equation (1) is for the top plate. A similar equation is obtained for the bottom plate with $\bar{w}_1$, a, a_{i1}, h_1, D_1 replaced by $\bar{w}_2$, b, b_{i2}, h_2, D_2. The double-plate system connected together by $(n-1)$ intermediate, elastic connections can be split up into a set of $2(n-1)$ annular plates of radii (b_1,b_2), $(b_2,b_3),\ldots(b_{j-1},b_j)\ldots(b_{n-1},a)$, and (b_{n-1},b) and two central complete plates of radii b_1 or two central annualr plates of radii (a_{i1},b_1) and (b_{i2},b_1). By matching the continuity conditions at the intermediate supports and satisfying the boundary conditions at the outer edges, the problem of buckling of the plate system can be solved. However, the solutions for the annular segments and for the center portion should be obtained separately before applying the continuity and edge conditions. These solutions are thus discussed in the following paragraphs.

For the case of annular plates, the inplane stresses existing at buckling are the same as the prebuckling stresses of an undeflected flat plate. The stress resultants $N_{\rho j1}$, $N_{\theta j1}$, and $N_{\rho\theta j1}$ existing in the jth plate (annular) have been obtained as

$$N_{\rho j1}=h_1\,\sigma_{\rho j1}=h_1\,[-A_1+A_2/\rho^2] \tag{2a}$$

$$N_{\theta j1}=h_1\,\sigma_{\theta j1}=h_1\,[-A_1-A_2/\rho^2] \tag{2b}$$

$$N_{\rho\theta j1}=h_1\,\tau_{\rho\theta j1}=0 \tag{2c}$$

When the plates have different loads on the inner and outer edges, the solutions are obtained as shown as follows. For the symmetric buckling of the jth annular plate, Eq. (1) will reduce to

$$\frac{d^4\bar{w}_{1j}}{d\rho^4}+\frac{2}{\rho}\frac{d^3\bar{w}_{1j}}{d\rho^3}-\frac{(1+\mu_{2j})}{\rho^2}\frac{d^2\bar{w}_{1j}}{\partial\rho^2}+\frac{(1+\mu_{2j})}{\rho^3}\frac{d\bar{w}_{1j}}{d\rho}+\mu_{1j}\left(\frac{d^2\bar{w}_{1j}}{d\rho^2}+\frac{1}{\rho}\frac{dw_{1j}}{d\rho}\right)=0 \tag{3}$$

Equation (3) can be factorized as

$$\left(\frac{d}{d\rho}+\frac{1}{\rho}\right)\left[\frac{d^3\bar{w}_{1j}}{d\rho^3}+\frac{1}{\rho}\frac{d^2\bar{w}_{1j}}{d\rho^2}-\frac{(1+\mu_{2j})}{\rho^2}\frac{d\bar{w}_{1j}}{d\rho}+\mu_{1j}\frac{d\bar{w}_{1j}}{d\rho}\right]=0 \tag{4}$$

The solution to Eq. (4) for the jth annular plate is [7-9]

$$\bar{w}_{1j}=A_{1j}\int_0^\rho S_{0,\wedge_1}(\mu_{1j}^{1/2}\rho)\,d\rho+A_{2j}\sum_{f=0}^{\infty}J(\wedge_1+2f+1)\,(\mu_{1j}^{1/2}\rho)+A_{3j}\sum_{f=0}^{\infty}J(-\wedge_1+2f+1)\,(\mu_{1j}^{1/2}\rho)+A_{j4} \tag{5}$$

where

$$\wedge_1=[1+\mu_{2j}]^{1/2} \tag{6}$$

$S_{0,\wedge_1}(\mu_{1j}^{1/2}\rho)$ represents Lommel's function of parameters 0 and $\wedge_1$ and argument $(\mu_{1j}^{1/2}\rho)$.

For the asymmetric mode Eq. (1) gives

$$\nabla^4\bar{w}_{1j}+\mu_{1j}\nabla^2\bar{w}_{1j}-\frac{\mu_{2j}}{\rho^2}\left(\frac{\partial^2\bar{w}_{1j}}{\partial\rho^2}-\frac{1}{\rho}\frac{\partial\bar{w}_{1j}}{\partial\rho}+\frac{1}{\rho^2}\frac{\partial^2\bar{w}_{1j}}{\partial\theta^2}\right)=0 \tag{7}$$

The deflection function may be assumed as

$$\bar{w}_{1j}=W_{1j}\cos m\theta \tag{8}$$

For the first asymmetric mode $(m=1)$, Eq. (7) reduces to

$$\frac{d^4W_{1j}}{d\rho^4}+\frac{2}{\rho}\frac{d^3W_{1j}}{\partial\rho^3}-\frac{(3+\mu_{2j})}{\rho^2}\frac{d^2W_{1j}}{d\rho^2}+\frac{(3+\mu_{2j})}{\rho^3}\frac{dW_{1j}}{d\rho}-\frac{(3+\mu_{2j})}{\rho^4}W_{1j}+\mu_{1j}\left(\frac{d^2W_{1j}}{d\rho^2}+\frac{1}{\rho}\frac{dW_{1j}}{d\rho}-\frac{1}{\rho^2}W_{1j}\right)=0 \tag{9}$$

Introducing a transformation

$$W_{1j}=\rho\bar{W}_{ij} \tag{10}$$

into Eq. (9) and reducing, it can be factorized as

$$\left(\frac{d}{d\rho}+\frac{3}{\rho}\right)\left[\frac{d^3\bar{W}_{1j}}{d\rho^3}+\frac{3}{\rho}\frac{d^2\bar{W}_{1j}}{d\rho^2}-\frac{(3+\mu_{2j})}{\rho^2}\frac{d\bar{W}_{1j}}{d\rho}+\mu_{ij}\frac{d\bar{W}_{1j}}{d\rho}\right]=0 \tag{11}$$

Solution to Eq. (11) is obtained as [7-9]

$$\bar{W}_{1j}=A_{1j}\int\!\!\int\rho^{-1}S_{-1,\alpha_1}(\mu_{1j}^{1/2}\rho)\,d\rho+A_{2j}\int\!\!\int\rho^{-1}J_{\alpha_1}(\mu_{1j}^{1/2}\rho)\,d\rho+A_{3j}\int\!\!\int\rho^{-1}J_{-\alpha_1}(\mu_{1j}^{1/2}\rho)\,d\rho+A_{4j} \tag{12}$$

where

$$\alpha_1 = (4+\mu_{2j})^{1/2} \tag{13}$$

Hence,

$$\bar{W}_{1j} = [A_{1j}\rho\int_0^\rho \rho^{-1} S_{-1,\alpha_1}(\mu_{1j}^{1/2}\rho)\,d\rho + A_{2j}\rho\int_0^\rho \rho^{-1} J_{\alpha 1}(\mu_{1j}^{1/2}\rho)\,d\rho + A_{3j}\rho\int_0^\rho \rho^{-1} J_{-\alpha_1}(\mu_{1j}^{1/2}\rho)\,d\rho + A_{4j}\rho]\cos\theta \tag{14}$$

For the higher modes ($m \geq 2$), the solution can be obtained as indicated below. If we assume the same deflection function given in Eq. (8) and substitute it into Eq. (1), it becomes

$$\frac{d^4W_{1j}}{d\rho^4} + \frac{2}{\rho}\frac{d^3W_{1j}}{d\rho^3} - \frac{(1+2m^2+\mu_{2j})}{\rho^2}\frac{d^2W_{1j}}{d\rho^2} + \frac{(1+2m^2+\mu_{2j})}{\rho^3}\frac{dW_{1j}}{d\rho} + \frac{(m^4-4m^2-\mu_{2j}m^2)}{\rho^4}W_{1j} + \mu_{1j}\left(\frac{d^2W_{1j}}{d\rho^2} + \frac{1}{\rho}\frac{dW_{1j}}{d\rho} - \frac{m^2}{\varphi^2}W_{1j}\right) = 0 \tag{15}$$

Equation (15) is transformed by using

$$\rho = e^u \tag{16}$$

and the resulting equation is

$$\frac{d^4W_{1j}}{du^4} - 4\frac{d^3W_{1j}}{du^3} + (4-2m^2-\mu_{2j})\frac{d^2W_{1j}}{du^2} + (4m^2+2\mu_{2j})\frac{dW_{1j}}{du} + (m^4-4m^2-\mu_{2j}m^2)W_{1j} + \mu_{1j}e^{2u}\left(\frac{d^2W_{1j}}{du^2} - m^2W_{1j}\right) = 0 \tag{17}$$

If we assume the solution in the form of the usual Frobenius series,

$$W_{1j} = \sum_{f=0,1}^{\infty} c_f e^{(p+2f)u} \tag{18}$$

substitute it into Eq. (17), and reduce it, the indicial equation

$$[p^4-4p^3+(4-2m^2-\mu_{2j})p^2+(4m^2+2\mu_{2j})p + (m^4-4m^2-\mu_{2j}m^2)]c_0 = 0 \tag{19}$$

is obtained, as well as the recurrence relations,

$$[(p+2)^4-4(p+2)^3+(4-2m^2-\mu_{2j})(p+2)^2 + (4+2\mu_{2j})(p+2)+(m^4-4m^2-\mu_{2j}m^2)]c_1 + d_{1j}(p^2-m^2)c_0 = 0 \tag{20a}$$

$$[(p+2f)^4-4(p+2f)^3+(4-2m^2-\mu_{2j})(p+2f)^2 + (4+2\mu_{2j})(p+2f)+(m^4-4m^2-\mu_{2j}m^2)]c_f + \mu_{1j}\{[p+2(f-1)]^2-m^2\}c_{f-1} = 0 \tag{20b}$$

The indical equation [Eq. (19)] is solved by any of the usual analytical methods, and the four roots p_1, p_2, p_3, and p_4 are determined. Then the solution to Eq. (1) for the case of annular isotropic plate with different edge loadings can be written as

$$\bar{w}_{1j} = [A_{1j}\phi_1(\mu_{1j},\mu_{2j},\rho) + A_{2j}\phi_2(\mu_{1j},\mu_{2j},\rho) + A_{3j}\phi_3(\mu_{1j},\mu_{2j},\rho) + A_{4j}\phi_4(\mu_{1j},\mu_{2j},\rho)]\cos m\theta \tag{21}$$

where

$$\phi_1(\mu_{1j},\mu_{2j},\rho) = \sum_{f=0,1}^{\infty} c_f \rho^{(p_1+2f)} \tag{22a}$$

$$\phi_2(\mu_{1j},\mu_{2j},\rho) = \sum_{f=0,1}^{\infty} c'_f \rho^{(p_2+2f)} \tag{22b}$$

$$\phi_3(\mu_{1j},\mu_{2j},\rho) = \sum_{f=0,1}^{\infty} c''_f \rho^{(p_3+2f)} \tag{22c}$$

$$\phi_4(\mu_{1j},\mu_{2j},\rho) = \sum_{f=0,1}^{\infty} c'''_f \rho^{(p_4+2f)} \tag{22d}$$

and the coefficients c_f are determined from the recurrence relations given in Eq. (20).

When the loads on both the edges are the same, the solutions given in Eqs. (22) reduce to known solutions in terms of Bessel function

$$\bar{w}_{1j} = [A_{1j}J_m(\mu^{1/2}\rho) + A_{2j}Y_m(\mu^{1/2}\rho) + A_{3j}\rho^m + A_{4j}\rho^{-m}]\cos m\theta \tag{23}$$

For the case of the central complete plate, Eq. (23) becomes

$$\bar{w}_{11} = [A_{11}J_m(\mu^{1/2}\rho) + A_{21}\rho^m]\cos m\theta \tag{24}$$

The solutions for the other $(n-1)$ annular portions of an annular continuous plate of $(n-2)$ annular portions and one central portion of a complete continuous plate are obtained from Eqs. (5, 14, 21, 23, and 24) by changing the arbitrary constants A_{1j}. A similar procedure may also be repeated for the bottom plate.

Boundary and Continuity Conditions

The solutions given in Eqs. (5, 14, 21, 23, and 24), also must satisfy the restraints imposed upon them by the intermediate supports and the boundaries. Besides the boundary conditions (which can be obtained from any standard textbook), the following continuity conditions must also be satisfied. At any intermediate support "j"

$$(\bar{w}_{1j})_{\rho_{j-}} = (\bar{w}_{1j})_{\rho_{j+}} \tag{25a}$$

$$(\bar{w}_{2j})_{\rho_{j-}} = (\bar{w}_{2j})_{\rho_{j+}} \tag{25b}$$

$$(\partial\bar{w}_{1j}/\partial\rho)_{\rho_{j-}} = (\partial\bar{w}_{1j}/\partial\rho)_{\rho_{j+}} \tag{25c}$$

$$(\partial\bar{w}_{2j}/\partial\rho)_{\rho_{j-}} = (\partial\bar{w}_{2j}/\partial\rho)_{\rho_{j+}} \tag{25d}$$

$$(M_{\rho 1})_{\rho_{j-}} = (M_{\rho 1})_{\rho_{j+}} \tag{25e}$$

$$(M_{\rho 2})_{\rho_{j-}} = (M_{\rho 2})_{\rho_{j+}} \tag{25f}$$

$$(V_{\rho 1j})_{\rho_{j+}} - (V_{\rho 1j})_{\rho_{j-}} = q\kappa_j[(\bar{w}_{1j})_{\rho_{j-}} - (\bar{w}_{2j})_{\rho_{j-}}] \tag{25g}$$

$$(V_{\rho 2j})_{\rho_{j+}} - (V_{\rho 2j})_{\rho_{j-}} = q\kappa_j s_1 (h_1/h_2)^3 d^3[(\bar{w}_{2j})_{\rho_{j-}} - (\bar{w}_{1j})_{\rho_{j-}}] \tag{25h}$$

Characteristic Determinants for Example Problems

For the purpose of numerical calculations, two specific problems shown in Fig. 2 will now be discussed in detail. Both the cases considered are for isotropic plate systems with one intermediate elastic ring support. The eigen determinant obtained for both the cases can be expressed as

$$[A_{i,j}] = 0,\ 1,\ j = 1,2,\ldots,\ 12 \tag{26}$$

For the case of a fixed-fixed double-plate system, the elements of the eigendeterminant given in Eq. (26) are

$$A_{1,1} = \left[\frac{(1-\nu_1)\ (m^2-m)}{\rho_s{}^2} - \mu\right] J_m(\mu^{1/2}\rho_s) + \frac{(1-\nu_1)\mu^{1/2}}{\rho_s} J_{m+1}(\mu^{1/2}\rho_s) \tag{27a}$$

$$A_{1,2} = (1-\nu_1)\ (m^2-m)\rho_s{}^{m-2} \tag{27b}$$

$$A_{1,3} = -A_{1,1} \tag{27c}$$

$$A_{1,4} = \left[\frac{(1-\nu_1)\ (m^2-m)}{\rho_s{}^2} - \mu\right] Y_m(\mu^{1/2}\rho_s) + \frac{(1-\nu_1)\mu^{1/2}}{\rho_s} Y_{m+1}(\mu^{1/2}\rho_s) \tag{27d}$$

$$A_{1,5} = -A_{1,2} \tag{27e}$$

$$A_{1,6} = \frac{(1-\nu_1)}{\rho_s{}^2} \quad (\text{for } m=0) \tag{27f}$$

$$A_{1,6} = -(1-\nu_1)\ (m^2+m)\rho_s{}^{-m-2} \quad (\text{for } m>0) \tag{27g}$$

$$A_{2,1} = \frac{m\ J_m(\mu^{1/2}\rho_s)}{\rho_s} - \mu^{1/2} J_{m+1}(\mu^{1/2}\rho_s) \tag{27h}$$

$$A_{2,2} = m\ \rho_s^{m-1} \tag{27i}$$

$$A_{2,3} = -A_{2,1} \tag{27j}$$

$$A_{2,4} = \left[\frac{m\ Y_m(\mu^{1/2}\rho_s)}{\rho_s}\right] - \mu^{1/2} Y_{m+1}(\mu^{1/2}\rho_s) \tag{27k}$$

$$A_{2,5} = -A_{2,2} \tag{27l}$$

$$A_{2,6} = -1/\rho_s \quad (\text{for } m=0) \tag{27m}$$

$$A_{2,6} = m\ \rho_s^{-m-1} \quad (\text{for } m>0) \tag{27n}$$

$$A_{3,1} = J_m(\mu^{1/2}\rho_s) \tag{27o}$$

$$A_{3,2} = \rho_s{}^m \tag{27p}$$

$$A_{3,3} = -A_{3,1} \tag{27q}$$

$$A_{3,4} = Y_m(\mu^{1/2}\rho_s) \tag{27r}$$

$$A_{3,5} = -A_{3,2} \tag{27s}$$

$$A_{3,6} = -\log(\rho_s) \quad (\text{for } m=0) \tag{27t}$$

$$A_{3,6} = -\rho_s{}^{-m} \quad (\text{for } m>0) \tag{27u}$$

$$A_{4,3} = J_m(\mu^{1/2}) \tag{27v}$$

$$A_{4,4} = Y_m(\mu^{1/2}) \tag{27w}$$

$$A_{4,5} = 1 \tag{27x}$$

$$A_{4,6} = 0 \quad (\text{for } m=0) \tag{27y}$$

$$A_{4,6} = 1 \quad (\text{for } m>0) \tag{27z}$$

$$A_{5,3} = m\ J_m(\mu^{1/2}) - \mu^{1/2} J_{m+1}(\mu^{1/2}) \tag{27a'}$$

$$A_{5,4} = m\ Y_m(\mu^{1/2}) - \mu^{1/2}\ Y_{m+1}(\mu^{1/2}) \tag{27b'}$$

$$A_{5,5} = m \tag{27c'}$$

$$A_{5,6} = 1 \quad (\text{for } m=0) \tag{27d'}$$

$$A_{5,6} = -m \quad (\text{for } m>0) \tag{27e'}$$

$$A_{6,1} = \left[\frac{(1-\nu_1)\ (m^3-m^2)}{\rho_s{}^3} + \frac{\mu_m}{\rho_s} + q\right] \times \frac{J_m(\mu^{1/2}\rho_s)}{q} - \left[\frac{(1-\nu_1)\mu^{1/2}m^2}{\rho_s{}^2} + \mu^{3/2}\right] \frac{J_m(\mu^{1/2}\rho_s)}{q} \tag{27f'}$$

$$A_{6,2} = \rho_s{}^m \tag{27g'}$$

$$A_{6,3} = \left[-\frac{(1-\nu_1)\ (m^3-m^2)}{\rho_s{}^3} - \frac{\mu_m}{\rho_s}\right] \frac{J_m(\mu^{1/2}\rho_s)}{q} + \left[\frac{(1-\nu_1)\mu^{1/2}m^2}{\rho_s{}^2} + \mu^{3/2}\right] \frac{J_m(\mu^{1/2}\rho_s)}{q} \tag{27h'}$$

$$A_{6,4} = \left[-\frac{(1-\nu_1)\ (m^3-m^2)}{\rho_s{}^3} - \frac{\mu_m}{\rho_s}\right] \frac{Y_m(\mu^{1/2}\rho_s)}{q} + \left[\frac{(1-\nu_1)\mu^{1/2}m^2}{\rho_s{}^2} + \mu^{3/2}\right] \frac{Y_m(\mu^{1/2}\rho_s)}{q} \tag{27i}$$

$$A_{6,7} = -J_m(\mu_2{}^{1/2}\rho_{s1}) \tag{27j'}$$

$$A_{6,8} = -\rho_{s1}{}^m \tag{27k'}$$

The elements

$A_{7,7}$, $A_{7,8}$, $A_{7,9}$, $A_{7,10}$, $A_{7,11}$, $A_{7,12}$, $A_{8,7}$,

$A_{8,8}$, $A_{8,9}$, $A_{8,10}$, $A_{8,11}$, $A_{8,12}$, $A_{9,7}$, $A_{9,8}$,

$A_{9,9}$, $A_{9,10}$, $A_{9,11}$, $A_{9,12}$, $A_{10,9}$, $A_{10,10}$, $A_{10,11}$,

$A_{10,12}$, $A_{11,9}$, $A_{11,10}$, $A_{11,11}$, $A_{11,12}$,

$A_{12,7}$, $A_{12,8}$, $A_{12,9}$, $A_{12,10}$, $A_{12,1}$, $A_{12,2}$

could be obtained from the elements

$A_{1,1}$, $A_{1,2}$, $A_{1,3}$, $A_{1,4}$, $A_{1,5}$, $A_{1,6}$

$A_{2,1}$, $A_{2,3}$, $A_{2,4}$, $A_{2,5}$, $A_{2,6}$, $A_{3,1}$, $A_{3,2}$,

$A_{3,3}$, $A_{3,4}$, $A_{3,5}$, $A_{3,6}$, $A_{4,3}$, $A_{4,4}$, $A_{4,5}$,

$A_{4,6}$, $A_{5,3}$, $A_{5,4}$, $A_{5,5}$, $A_{5,6}$, $A_{6,1}$,

$A_{6,2}$, $A_{6,3}$, $A_{6,4}$, $A_{6,7}$, $A_{6,8}$,

respectively, by replacing μ, ν_1, ρ_{s1}, and ρ_s by μ_2, ν_2, ρ_s, and ρ_{s1}, respectively. All the other elements of the eigen determinant are zero.

For the case of a fixed-free double-plate system, all the elements of the foregoing eigen determinant except $A_{10,9}$, $A_{10,10}$, $A_{10,11}$, $A_{10,12}$, $A_{11,9}$, $A_{11,10}$, $A_{11,11}$, $A_{11,12}$ are the same.

These elements are

$$A_{10,9}=[(1-\nu_2)\ (m^2-m)-\mu_2]J_m[\mu_2{}^{1/2}) + (1-\nu_2)\mu_2{}^{1/2}\ J_{m+1}(\mu_2{}^{1/2}) \quad (28a)$$

$$A_{10,10}=[(1-\nu_2)\ (m^2-m)-\mu_2]\,Y_m(\mu_2{}^{1/2}) + (1-\nu_2)\mu_2{}^{1/2}\ Y_{m+1}(\mu_2{}^{1/2}) \quad (28b)$$

$$A_{10,11}=(1-\nu_2)\ (m^2-m) \quad (28c)$$

$$A_{10,12}=(1-\nu_2)\ (m^2+m) \quad (28d)$$

$$A_{11,9}=[-(1-\nu_2)\ (m^3-m^2)-\mu_2 m]J_m(\mu_2{}^{1/2}) + [(1-\nu_2)\mu_2{}^{1/2}\ m^2+\mu_2{}^{3/2}]J_{m+1}(\mu_2{}^{1/2}) \quad (28e)$$

$$A_{11,10}=[-(1-\nu_2)\ (m^3-m^2)-\mu_2 m]\,Y_m(\mu_2{}^{1/2}) + [(1-\nu_2)\mu_2{}^{1/2}\ m^2+\mu_2{}^{3/2}]\,Y_{m+1}(\mu_2{}^{1/2}) \quad (28f)$$

$$A_{11,11}=-(1-\nu_2)\ (m^3-m^2) \quad (28g)$$

$$A_{11,12}=0 \quad (\text{for } m=0) \quad (28h)$$

$$A_{11,12}=(1-\nu_2)\ (m^3+m^2) \quad (\text{for } m>0) \quad (28i)$$

Numerical results obtained for specific problems shown in Fig. 2 are given in Figs. 3-13. As stated before,[6] the continuity conditions of bending moment and shear associated with these problems could be effectively replaced by the second and third derivatives of the deflection function $\bar{w}_1$ or $\bar{w}_2$ with respect to ρ. The parameters which influence the buckling parameter μ are the thickness ratio h_1/h_2, the load ratio N_2/N_1, the ratio of Young's moduli, the ratio of plates radii b/a, the distance ρ_s of the elastic support from the center, and the elasticity of the support measured as the coefficient of elasticity of the support q.

Figure 3 illustrates the influence of the thickness ratio on the symmetric buckling loads for the case of a fixed-fixed plate system. When $h_1/h_2 \neq 1$, the system behaves as a single unit when it buckles; always the elasticity of the support has a definite influence on the buckling loads. However, when

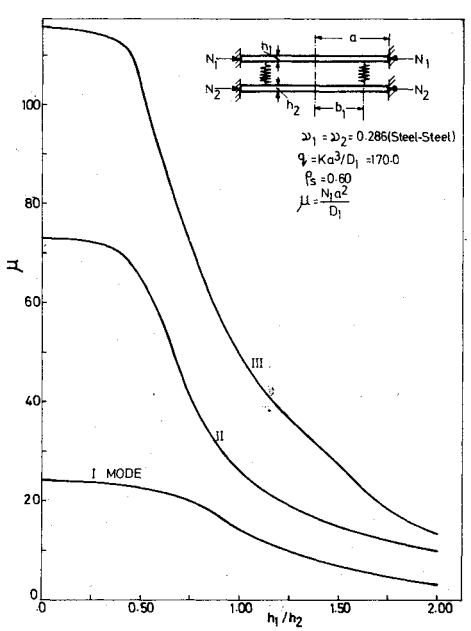

Fig. 3 Effect of thickness ratio on symmetric buckling loads of a continuous double plate system with fixed ends (uniform loading $N_2/N_1=1.0$).

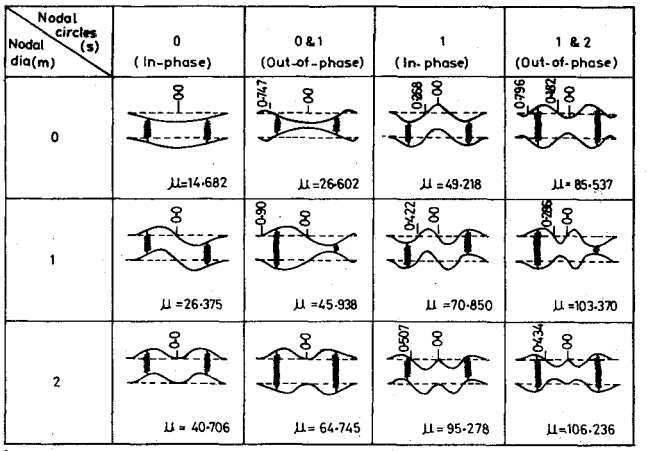

Fig. 4 Buckling modes of continuous double-plate system on an elastic support with fixed-fixed edges-identical plates ($\nu_1=\nu_2=0.286$, $q=170.0$, $N_2/N_1=1.00$, $\rho_s=0.60$).

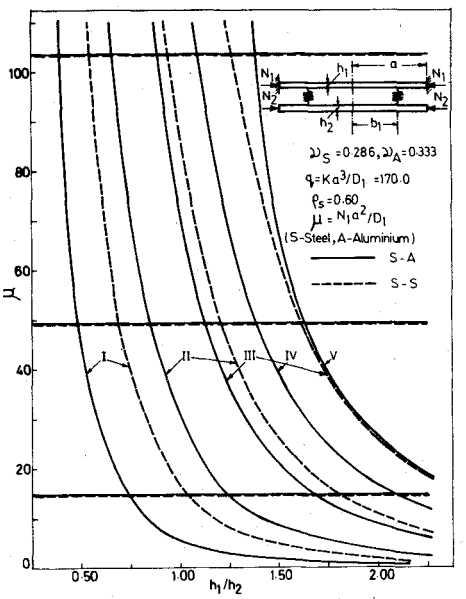

Fig. 5 Effect of thickness ratio on the symmetric buckling loads of a continuous double plate system with fixed-free edges (uniform loading $N_2/N_2=1.0$).

$h_1/h_2=1$, the behavior can be separated into two types, in one of which the system acts as though made up of two individual plates without the support elasticity contributing to it and in the other of which the system behaves as a single unit. Hence, in the former case the buckling loads are the same as for a single plate. When $h_1/h_2=0$, this represents the case of a single continuous plate with fixed ends and on elastic supports. It is found that the results check well with the results given in Ref. 6. As h_1/h_2 increases, the buckling parameter decreases since the combined stiffness of the system also decreases; because μ is dependent on N_1 and D_1 of the top plate, the D_2 of the bottom plate goes on decreasing from infinity to zero as h_1/h_2 increases from zero to infinity. Figure 4 shows some of the interesting modes of the double-plate system with fixed-fixed edges when the plates are identical.

Figure 5 indicates the influence of the thickness ratio h_1/h_2 on the symmetric buckling loads for steel-steel and steel-aluminium combinations of a double-plate system with fixed-free edges; the bottom plate is assumed to be aluminium in the steel-aluminium combination. Two distinct types of buckling behavior are observed; in one case, the free plate and the elastic ring connections (supports) do not influence the buckling of the system; in this case the buckling load of the

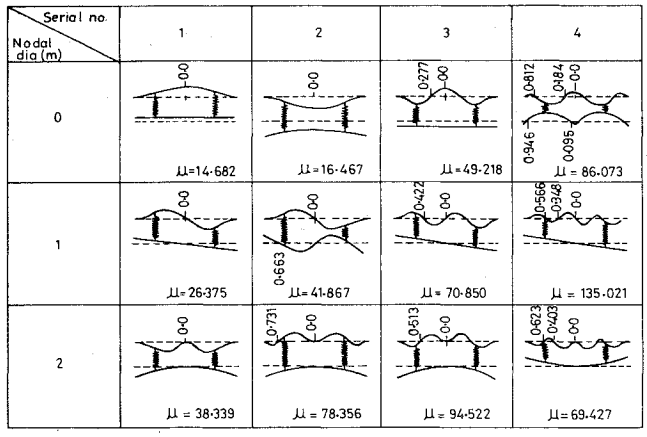

Fig. 6 Buckling modes of a continuous double-plate system on an elastic support with fixed-free edges-identical plates ($\nu_1 = \nu_2 = 0.286$, $q = 170.0$, $N_2/N_1 = 1.0$, $\rho_s = 0.60$).

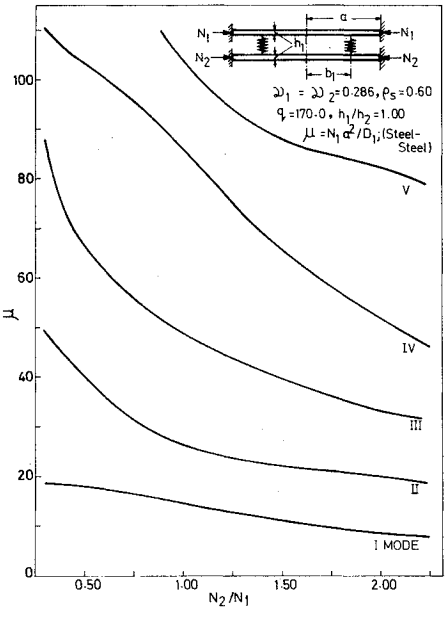

Fig. 7 Critical buckling loads of a continuous double plate system on elastic supports with fixed-fixed edges under proportional loading-symmetric modes.

system represents the buckling load of the top single plate. In the other case, the system acts as a whole and all the three elements of the system, namely, the top plate, the bottom plate, and the elastic ring support, contribute to the buckling behavior of the system. In the first case, the bottom plate moves only as a rigid body, but in the second case both the plates get buckled. For the steel-aluminium combination, when $h_1/h_2 > 0.74$, the lowest mode is the coupled mode; below that ratio, the lowest mode is due to the buckling of the single fixed plate. For the steel-steel combination, when $h_1/h_2 > 1.04$, the lowest mode is the coupled mode. As h_1/h_2 increases, the coupled mode goes on decreasing, owing to the reasons stated before for the cases of fixed-fixed plates. When $h_1/h_2 = 1$, the system buckles in two ways, in one case it buckles as a single fixed plate and in the other case it buckles as a coupled system. The resulting of the coupled system are the same as those of free continuous plates on elastic (also rigid when $m = 0$ and $m = 1$) supports.The reason is obvious, at the buckling point the elastic ring support gets a rigid body displacement which makes it a rigid support and then the bottom plate buckles (along with the top plate) as a single plate on a rigid ring support. The rigid body displacements and the coupled buckling behavior can be clearly observed in the figures given in Fig. 6.

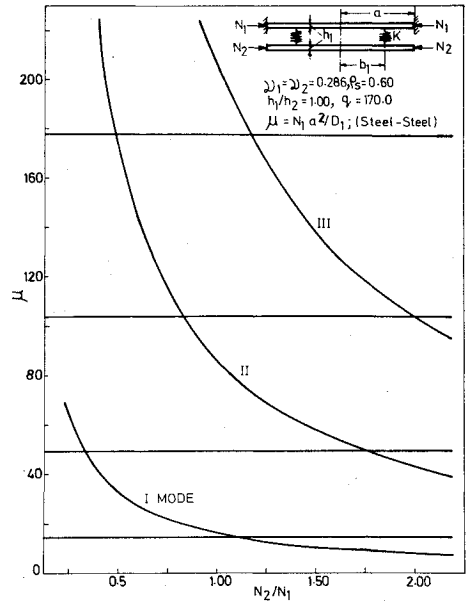

Fig. 8 Critical buckling loads of a continuous double plate system on elastic supports with fixed-free edges under proportional loading-symmetric modes

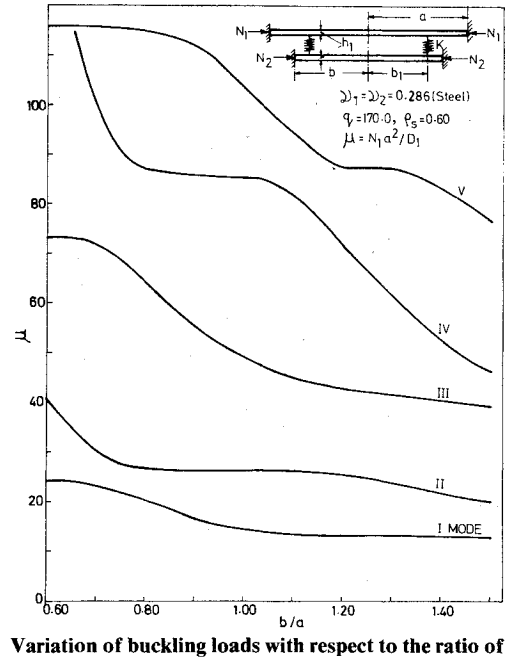

Fig. 9 Variation of buckling loads with respect to the ratio of radii of plates with fixed-fixed edges of a continuous double-plate system on elastic supports (uniform loading $N_2/N_1 = 1.00$; symmetric modes).

Figures 7 and 8 illustrate the influence of the load ratio N_2/N_1 on the buckling of a fixed-fixed and fixed-free double plate system with identical plates. In Fig. 7 when $N_2/N_1 = 1.0$, the results are the same as obtained in Fig. 3 when $h_1/h_2 = 1.0$. The same observation holds good with regard to Figs. 5 and 8. Two distinct types of behavior can be observed in Fig. 8, for the case of the fixed-free double-plate system; one in which the single fixed plate (top) buckles and the other in which the complete system buckles. When $N_2/N_1 > 1.13$, the coupled buckling mode is lowest; below the load ratio, the single fixed-plate buckling mode is lowest.

The influence the ratio of the radii of the two plates on the buckling of the fixed-fixed and fixed-free double-plate system is given in Figs. 9 and 10. When $b/a = 1$, the results of Figs. 9 and 10 check with the respective values of Figs. 3 and 5, when $h_1/h_2 = 1.0$. Also when $b/a = 0.6$, the plate system buckles in

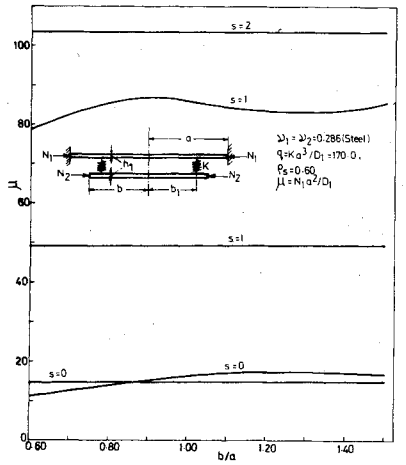

Fig. 10 Variation of buckling loads with respect to the ratio of radii of plates with fixed-free edges of a continuous double-plate system on elastic supports (uniform loading- $N_2/N_1=1.0$; symmetric modes).

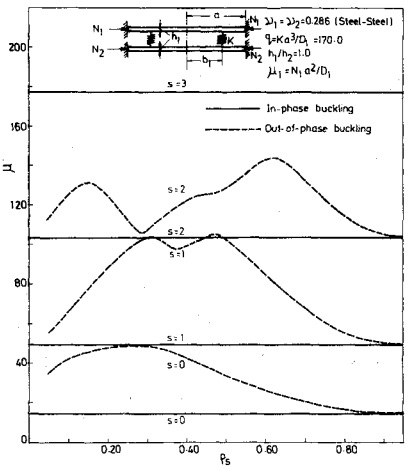

Fig. 11 Influence of support radius on symmetric buckling loads of elastically supported continuous double-plate system with fixed-fixed edges (uniform loading- $N_2/N_1=1.0$).

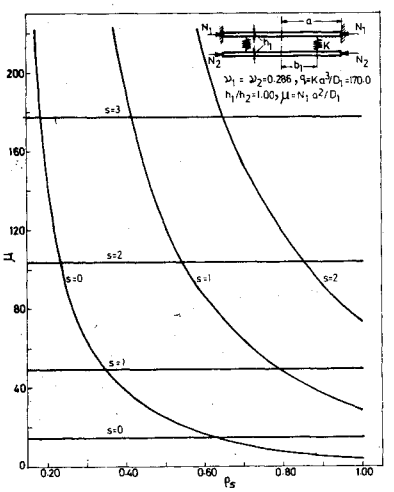

Fig. 12 Influence of support on symmetric buckling loads of elastically supported continuous double plate system with fixed-free edges (uniform loading- $N_2N_1=1.0$).

two ways. In Fig. 9 the lower part buckles as a single clamped plate with a plate radius of 0.6; the upper plate buckles as a clamped continuous plate on an elastic support and these values check with those given in Ref. 6 ($b/a=0.60$). In Fig. 10, the lower plate buckles as a single plate of radius 0.6 a with elastic simple supports; the top plate buckles as a clamped plate of radius "a" with no intermediate support ($b/a=0.60$).

Figures 11 and 12 give the influence of the position of the support on the buckling loads. In Fig. 11 ρ_s vs μ is plotted for a fixed-fixed plate system. When the plates are identical, there are two distinct types of buckling, in one of which the elastic support does not have any say and in the other of which the buckling loads are definitely influenced by the properties of the two plates and the elasticity of the support. We can call

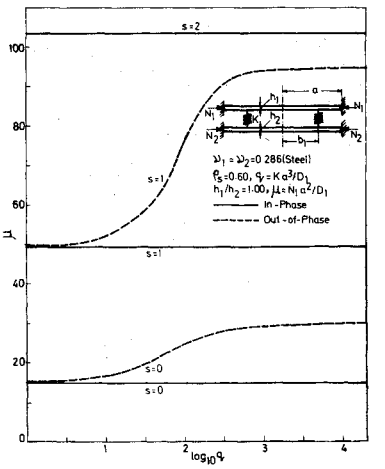

Fig. 13 Influence of support elasticity on the symmetric buckling loads of identical plates system with fixed-fixed edges (uniform loading- $N_2/N_1=1.00$).

them in-phase or out-of-phase buckling, respectively. It is found that when the plates and the loading are identical, the in-phase buckling gives the lowest buckling load. The buckling resistance of the system is maximum when $\rho_s=0.275$. In the case of fixed-free plates shown in Fig. 12, we have two types of buckling, the first in which the elasticity of the support does not influence the buckling loads and the other in which the system—the two plates and the elastic support—acts as integral one. In the second case, the buckling loads are the same as that given in Ref. 6 for plates on rigid supports ($m=0$). It is found that, when $\rho_s<0.625$, the lowest buckling loads are obtained as the buckling load of a plate with clamped edges; for ρ_s greater than 0.625, the lowest buckling load is given by the coupled motion.

The influence of the elasticity of the support on the buckling loads is shown in Fig. 13 as $\log_{10}\alpha$ vs μ for a fixed-fixed plate with identical plates. Once again the in-phase and out-of-phase buckling modes are observed. It is found that when the coefficient of support elasticity q tends to be zero, the buckling load is equivalent to that of a single plate with clamped edges; both the in-phase and out-of-phase modes merge together. When q becomes very large namely, $\log_{10} q>4$, (i.e., $q>10{,}000$) the buckling loads approach a limit asymptotically, which give the buckling loads of a double-plate system with an intermediate rigid support. Also, as observed beore, in a fixed-fixed plate system the first in-phase buckling load is the lowest buckling load of the system.

References

[1] Schleicher, F., "Die Knickspannungen von Eigenspannten Rechtekigen Platen," *Mitteilungen aus den Forschungsanstalten des Gutehoffnungshute-Koncerns,* Vol. 1, 1931.

[2] Schleicher, F., "Final Report of the First Congress of the International Association of Bridge and Structural Engineers," Paris, 1932, pp. 123.

[3] Bleich, F., *Buckling Strength of Metal Structures,* McGraw-Hill, New York, 1952, pp. 441-450.

[4] Norris, C. H., Polychrone, D. A., and Copozzoli, L. S., "Buckling of Intermittenly Supported Rectanglular Plates" *Welding Journal*, Vol. 30, Nov. 1951, pp. 546-556.

[5] Wittrick, W. H. and Curzon, P. L. V., "Buckling of a Flat Panel with a Series of Equidistant Longitundinal Supports in Combined Longitudinal Compression and Shear," *Aeronautical Quarterly*Vol. 20, Feb. 1969, pp. 17-24.

[6] Swamidas, A. S. J and Kunukkasseril, V. X., "Buckling of Continuous Circular Plates," *Transactions of the American Society of Civil Engineers*, Engineering Mechanics Div., Vol. 99, Aug. 1973 pp. 835-852.

[7] Erdelyi, E., Magnus, W., Oberhettinger, F., and Tricomi, F. G., *Higher Transcendental Functions*, Vol. 2, McGraw-Hill, New York, 1953, p. 40-47.

[8] Kamke, E., *Differential Gleichungen Lošungmethoden and Lošungen,* 3rd ed., Chelsea Pub. Co., New York, 1959, pp. 437-442.

[9] Majumdar, S., "Buckling of a Thin Annular Plate Under Uniform Compression," *AIAA Journal*, Vol. 9, Sept. 1971, pp. 1701-1707.